Computers & Geosciences 48 (2012) 41–49

Contents lists available at SciVerse ScienceDirect

Computers & Geosciences

journal homepage: www.elsevier.com/locate/cageo

Comparison of drainage-constrained methods for DEM generalization

Yumin Chen [a,*], John P. Wilson [b], Quansheng Zhu [a], Qiming Zhou [c]

[a] School of Resource and Environment Science, Wuhan University, 129 Luoyu Road, Wuhan, 430079, China
[b] Spatial Sciences Institute, University of Southern California, Los Angeles, CA 90089-0374, USA
[c] Department of Geography, Hong Kong Baptist University, Kowloon Tong, Kowloon, Hong Kong

ARTICLE INFO

Article history:
Received 13 February 2012
Received in revised form
1 May 2012
Accepted 3 May 2012
Available online 14 May 2012

Keywords:
Digital terrain modeling
Digital terrain analysis
DEM generalization
TINs
Drainage-constrained methods

ABSTRACT

In multi-scale digital terrain analysis, the main goal is to preserve the basic 'skeleton' with changing scales and to deliver more consistent measurements of terrain parameters at different scales. The drainage lines serve the basic morphology features and 'skeleton' in a basin, and therefore play an important role for most applications. Many drainage-constrained methods for DEM generalization have been proposed over the last few decades. This article compares three drainage-constrained methods: a Stream Burning algorithm, the ANUDEM algorithm as an example of a surface fitting approach, and the Compound method as an example of a constrained-TIN approach. All of these methods can be used to build coarser-scale DEMs while taking drainage features into account. The accuracy of the elevations and several terrain derivatives (slope, surface roughness) in the new digital terrain models along with the geometry or shape of key terrain features (streamline matching rate, streamline matching error) is then compared with each other to analyze the efficacy of these methods. The results show that the Compound algorithm offers the best performance over a series of generalization experiments.

1. Introduction

DEM generalization has been widely used in multi-scale digital terrain analysis. When a coarser analytical scale is required, the original finer-resolution DEM is generalized to establish a new DEM with a different resolution. At the same time, the terrain parameters and derivatives such as slope, aspect, curvature and drainage patterns may subsequently change (Zhang et al., 1999; Wilson and Gallant, 2000; Zhou and Liu, 2004; Tay et al., 2005).

One of the most widely used methods for DEM generalization is a resampling method, which requires averaging the neighboring cells of a high-resolution, square-grid DEM into a series of lower-resolution data sets (Wolock and Price, 1994; Kienzle, 2004; Li, 2008). This method will inevitably have a smoothing effect. Another common approach is to construct a multi-level Triangulated Irregular Network (TIN) using critical points and integral lines to represent the multi-scale digital terrain surface (Wu and Amaratunga, 2003; Danovaro et al., 2006). However, these methods often change the terrain features and derivatives when the DEM resolution is changed (Wilson and Gallant, 2000; Wu et al., 2008; Zhou and Chen, 2011).

In many practical applications, the goal is to retain significant terrain features, such as peaks, saddles, valley, ridge and drainage lines for coarser scale digital terrain analysis, and to deliver more consistent measurements of terrain parameters at different scales. Therefore, a 'morphology-based' approach is proposed, which takes important topographic features into account and retains the fundamental geomorphological and drainage features while changing scales (Weibel, 1992; Gesch, 1999; Soille et al., 2003).

The role and character of drainage enforcement in digital terrain analysis has evolved since Jenson and Domingue (1988) first proposed the notion. However, the drainage lines still constitute the basic morphology features and 'skeleton' in a basin, and therefore play an important role in all of the 'morphology-based' approaches. Numerous works over the last few decades have proposed drainage-constrained methods for DEM generalization (e.g. Southard, 1991; Zakšek and Podobnikar, 2005; Vázquez and Pascual, 2008). The main algorithms that focus on drainage or stream lines can be categorized into three groups: stream burning, surface fitting, and constrained-TIN algorithms.

A 'stream burning algorithm' can improve the replication of stream positions by using a raster representation of a vector stream network to trench known hydrological features into a DEM at a user-specified depth (Saunders, 2000; Callow et al., 2007). The advantages of this method are its simplicity, computational efficiency and tendency for the changes to affect fewer cells in the landscape. However, stream burning also creates a

* Corrresponding author. Tel.: (+86)27 68778386.
E-mail addresses: ymchen@whu.edu.cn (Y. Chen), jpwilson@usc.edu (J.P. Wilson).

0098-3004/$ - see front matter © 2012 Elsevier Ltd. All rights reserved.
http://dx.doi.org/10.1016/j.cageo.2012.05.002

discrepancy between the original DEM and the trenched 'stream' cells, leading to dramatic jumps in elevation, which are likely to affect derived properties such as slope, particularly when a deep trench is required to retain the preferred drainage lines.

Taking this idea one step further, more elaborate surface fitting or interpolation methods can be used to fit the terrain surface. A typical 'surface fitting approach' is the ANUDEM algorithm (Hutchinson, 1989), which utilizes irregularly spaced elevation data points (spot heights) and/or contour lines, streamlines, and an iterative finite difference interpolation technique to generate grid-based DEMs with few or no sinks. However, ANUDEM may alter the entire DEM to eliminate abrupt jumps between stream and non-stream cells (Callow et al., 2007), and this interpolation method may not produce optimal results if poor input data are selected (Wise, 2000). Another example is the fractal-based method proposed by Belhadj and Audibert (2005). A skeleton of the ridge and river networks is computed and stored in a DEM as initial values, and the elevation data set is enriched using a novel interpolation method based on a Midpoint Displacement Inverse process. More recently, Ai and Li (2010) proposed a structured analysis method to generalize DEM data through the identification of minor valleys and filling the corresponding depressions. With this approach, the unimportant valley branches are detected based on hydrologic significance and the elevations of the grid cells in these areas are raised to smooth the terrain surface.

The third approach utilizes TINs rather than the square-grid DEMs used in the first two approaches. Some of the earliest studies on TINs focused on the automated selection of significant features to construct the TIN models, such as the peaks, pits, passes, and points along ridge and channel lines and other breaks of slope (Peucker and Douglas, 1975; Fowler and Little, 1979; Heller, 1990; Lee, 1991). Douglas (1986) recommended using a 'richline' structure, in which the 'rich' lines referred to ridge and drainage lines that contain a large amount of information about the shape of the surface, for storing elevation data. Nelson et al. (1999) proposed a tessellation algorithm for automatically creating TINs from a set of GIS objects that correspond to the drainage features. Kidner et al. (2000) proposed a Multiscale Implicit Triangulated Irregular Network to generate triangulated terrain models that adapt their content and level of detail to the user's requirements. This implicit TIN only stores the vertices explicitly, together with linear constraints, such as cliffs and ridge lines. Danovaro et al. (2006) later proposed a Multi-resolution Surface Network (MSN), which used critical points (minima, maxima, saddle points) and integral lines to construct multi-resolution TINs. Finally, Zhou and Chen (2011) have proposed a compound method, which reconstructs the grid-based surface elevation data to construct a drainage-constrained TIN that is optimized to keep the important terrain features and slope morphology with the minimum number of sample points.

This article, therefore, investigates the efficacy of three of the aforementioned drainage-constrained methods for generating lower resolution DEMs. The Stream Burning algorithm of Saunders (2000), the ANUDEM algorithm (Hutchinson, 1989) as an example of a surface fitting approach, and the Compound method (Zhou and Chen, 2011) as an example of a constrained-TIN approach were used to build coarser-scale DEMs of the same area, and the elevations and various terrain derivatives were compared with one another to evaluate the effectiveness and suitability of these methods.

2. Methodology and data Sources

We selected three different high-resolution DEMs, with resolutions of 3, 10 and 30 m, respectively, to investigate the effect of original resolution on DEM generalization. The 10 m and 30 m DEMs cover the same area in southwestern Oregon (43.15–43.48° N, 123.67–124.12° W) in which the elevation ranged from 5 to 920 m (Fig. 1). The 10 m DEM is composed of 3,600 × 3,600 grid cells, while the 30 m DEM is composed of 1,200 × 1,200 grid cells. The 3 m DEM covered part of the same area (4,000 × 4,000 grid cells; 43.22–43.33° N, 123.88–124.03° W) and the elevation ranged from 44 to 760 m.

In the test, the original DEM was generalized to generate DEMs with different spatial resolutions, such that the 3 m DEM was resampled to 10, 30, 50, 90, 125, and 150 m spatial resolutions, the 10 m DEM was resampled to 30, 50, 90, 125, 150, and 250 m spatial resolutions, and the 30 m DEM was resampled to 50, 90, 125, 150, 250 and 500 m spatial resolutions, respectively. The drainage network was retrieved from the original DEMs using the simple "D8" flow routing algorithm (Mark, 1984) and it was further generalized using the Douglas–Peucker algorithm (Douglas and Peucker, 1973) with a threshold value of 3 m (up to 10 m resolution), 10 m (from 10 to 30 m resolution), 30 m (from 30 to 50 m resolution) and 50 m (for resolutions coarser than 50 m) to match the scale of the generated DEMs.

For the Stream Burning algorithm, the drainage network was generalized to the preferred scale and then rasterized using the "line to raster" command in ArcGIS 9.3. The stream lines were burned to the generalized DEMs by subtracting the descending depth (i.e. 10 m) along the drainage network from the respective DEM.

For the ANUDEM and Compound methods, the same significant points (e.g. peak or ridge points) and drainage network were used to ensure a fair comparison. Significant points were retrieved by the maximum z-tolerance algorithm (Heller, 1990; Chang, 2007), which relies on an iterative process starting with only two triangles, and then inserting a point with the largest elevation difference between the original DEM and TIN surface to reconstruct the TIN on each pass, until no point remains with a larger difference than some pre-determined threshold. The USGS DEM data accuracy standard in which a RMSE of one-half contour interval is the maximum permitted guided the specification of *z*-tolerance values at different scales (Table 1). These two algorithms used the same drainage network at each specified scale as the Stream Burning algorithm.

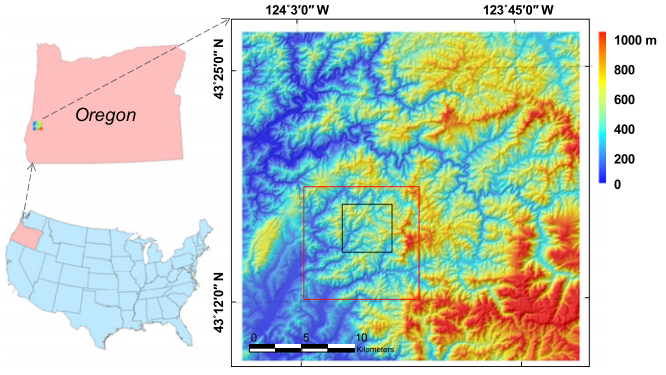

Fig. 1. The original 10 m and 30 m DEM used in this study (3600 × 3600 cells, 10 m cell size; 1200 × 1200 cells, 30 m cell size). The red box indicates the area of the original 3 m DEM (4000 × 4000 cells), and the black box indicates the area reproduced in Figs. 3–7. (For interpretation of the references to colour in this figure legend, the reader is referred to the web version of this article.)

Table 1
The spatial resolution and corresponding *z*-tolerance values.

Resolution (*m*)	10	30	50	90	125	150	250	500
Z-tolerance value (m)	8	20	30	50	70	90	130	180

For the ANUDEM algorithm, the significant points and drainage networks at a specified scale were interpolated in the DEM using the "topo to raster" command in ArcGIS 9.3, while the Compound method supplemented the maximum z-tolerance algorithm with additional drainage feature points and embedded streamlines to generate a drainage-constrained TIN.

The evaluation considered the accuracy of the new digital terrain models and selected terrain derivatives along with the geometry or shape of key terrain features, such as the shape of the drainage network. Therefore, the comparison was composed of three parts: namely, comparison of RMSEs, mean slope and surface roughness, and the streamline matching rate (SMR) and streamline matching error (SME).

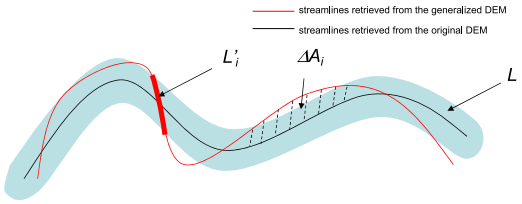

Fig. 2. The streamline matching rate (SMR) and streamline matching error (SME). The black lines denote streamlines retrieved from the original DEM, and the red lines denote streamlines retrieved from the generalized DEM. (For interpretation of the references to colour in this figure legend, the reader is referred to the web version of this article.)

2.1. Comparison of RMSE

The root mean square error (RMSE) is a good measure of the accuracy of the original and generalized elevation surfaces produced with the aforementioned algorithms, and can be computed as follows:

$$RMSE = \sqrt{\frac{\sum_{i=1}^{n}(Z'_i - Z_i)^2}{n}} \quad (1)$$

where Z denotes the elevation value of the original DEM, Z' denotes the elevation value of the generalized DEM or TIN, i denotes the ith unit, and n denotes the total number of units. The unit is the grid cell of the original DEM, and Z' is computed from the generalized DEM or TIN at the center of each grid of the original DEM.

2.2. Comparison of mean slope and surface roughness

The mean slope ($\bar{S}$) and surface roughness (K) were also used to compare the generalized DEMs created at varying scales with the aforementioned algorithms, and can be specified as followed:

$$\bar{S} = \frac{\sum_{i=1}^{n} S_i \times A_i}{\sum_{i=1}^{n} A_i} \quad (2)$$

$$K = \frac{A'}{A} = \frac{\sum_{i=1}^{n} A_i \sec S_i}{\sum_{i=1}^{n} A_i} \quad (3)$$

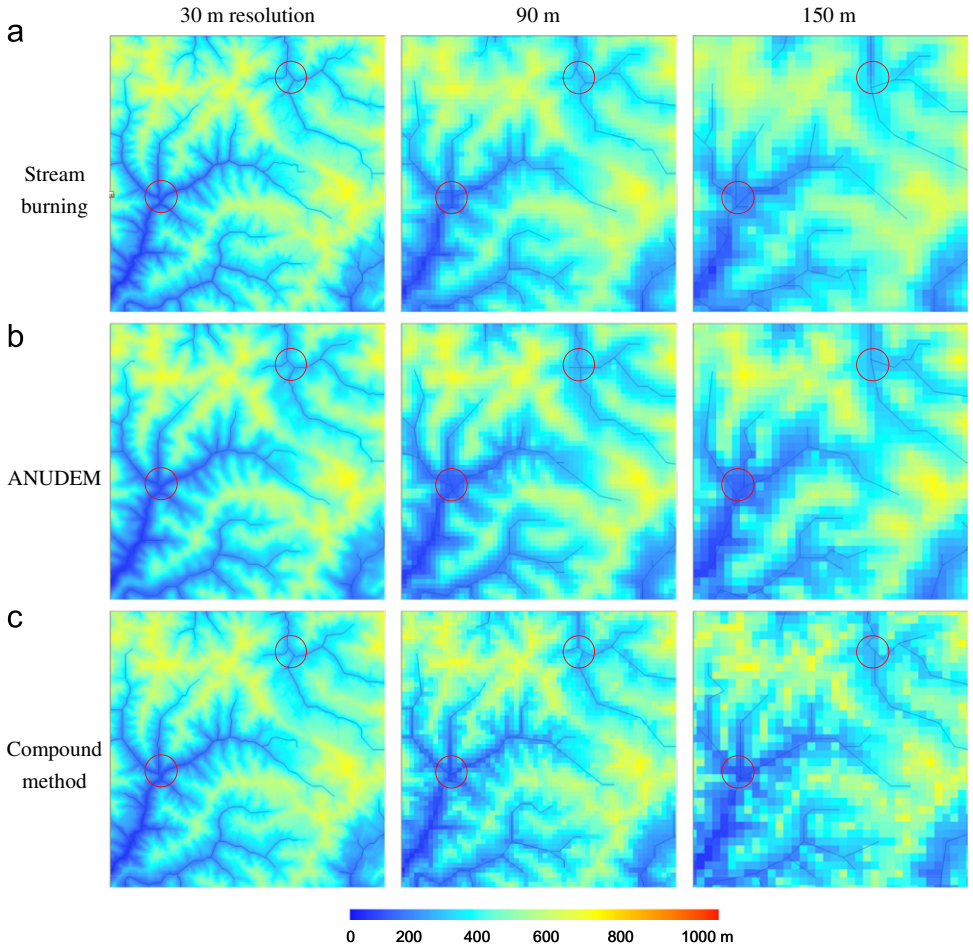

Fig. 3. Generalized DEMs generated from original 3 m DEM by three methods. The blue lines indicate the extracted drainage networks and the red circles indicate the places where morphological changes between the different methods are evident. (For interpretation of the references to colour in this figure legend, the reader is referred to the web version of this article.)

where S denotes the slope, A denotes the projected area (i.e. two-dimensional horizontal (planimetric) area of the DEM), A' denotes the surface area (i.e. the exposed (sloping) area of the DEM), i denotes the ith unit, and n denotes the total number of units.

2.3. Comparison of SMR and SME

The streamline matching rate (SMR) and streamline matching error (SME) show how well the drainage features were retained (Zhou and Chen, 2011). The SMR specifies the rate of the changes in the lengths of the drainage network or the similarity of the shape between the original and generalized DEM, while the SME measures the average dispersion between the features, and therefore represents the average streamline matching error (Fig. 2). To compute the SMR and SME, stream buffers were generated with widths matching the original DEM resolution and the resultant buffer zones were overlaid with the streamlines retrieved from the generalized DEM. We used these two factors to compare the shape of the drainage network for the generalized DEMs derived with the aforementioned algorithms, as follows:

$$SMR = \frac{L'}{L} \times 100 \quad (4)$$

$$SME = \frac{\Delta A}{L} \quad (5)$$

where the units of SMR and SME are percentages and meters, respectively, L' denotes the length of streamlines that fell into the corresponding stream buffer zones, L is the total length of the streamlines, and ΔA is the area of 'sliver' polygons between the streamlines retrieved from the original and generalized DEM.

3. Results and discussion

3.1. Comparison of RMSE

Figs. 3 and 4 show three examples of the coarser resolution DEMs generated with the selected methods from the original 3 and 30 m DEMs, respectively. There is a steady loss of clarity and detail as the DEM resolution is relaxed. The results from using the stream burning method reproduced in Figs. 3a and 4a show the tendency for this approach to retain the drainage network in the coarser DEMs. The smoothing effects of the surface fitting approach of ANUDEM are evident in Figs. 3b and 4b which also show how some of the detailed morphological features were quickly lost with this particular method. Figs. 3c and 4c, on the other hand, show how the main skeleton and some details in each of the DEM were retained better with the Compound method.

This assessment is confirmed by Table 2, which shows that the ANUDEM method always produced the largest RMSE values for the generalized DEMs, while the Compound method produced the lowest RMSE values for all six DEMs generalized from the 3 m DEM and four of six of the DEMs generated from the 10 and 30 m DEMs. The Stream Burning algorithm produced the lowest RMSEs

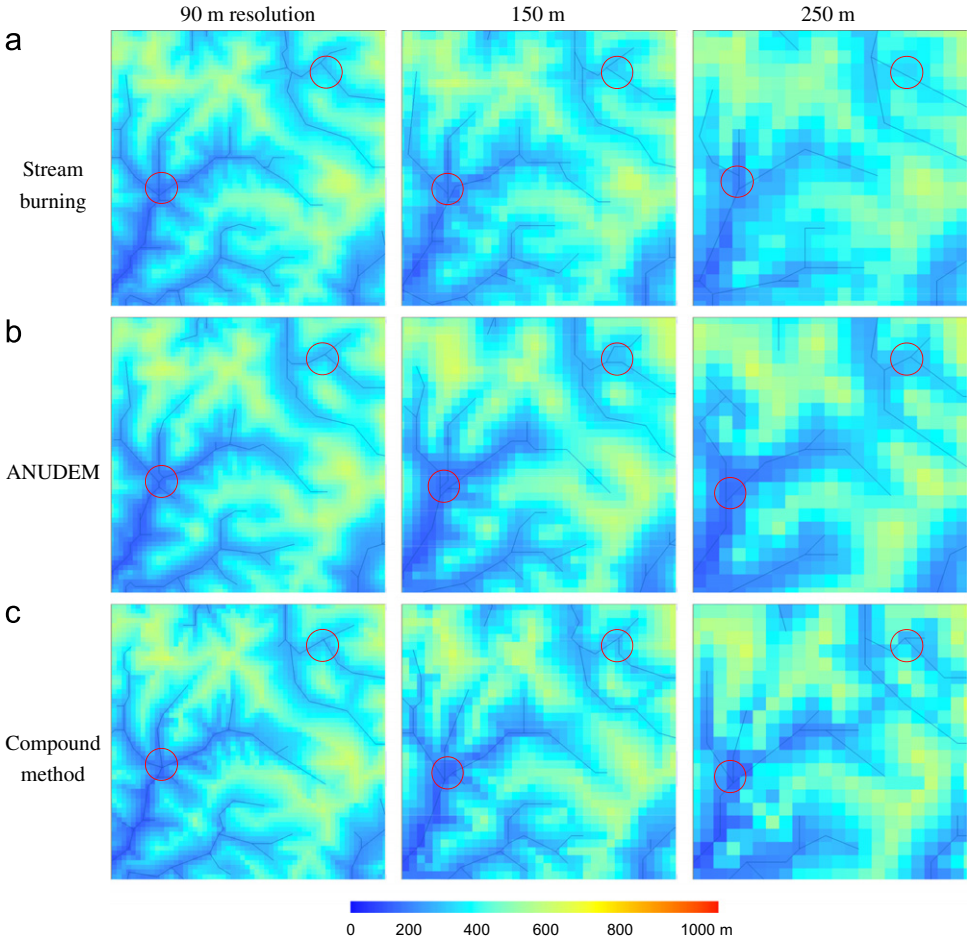

Fig. 4. Generalized DEMs generated from original 30 m DEM by three methods. The blue lines indicate the extracted drainage networks and the red circles indicate the places where morphological changes between the different methods are evident. (For interpretation of the references to colour in this figure legend, the reader is referred to the web version of this article.)

for the first two generalizations from the 10 and 30 m DEMs but was passed by the Compound method because the RMSE values from the Stream Burning algorithm increased more quickly (i.e. 9.7 times vs. 6.2 times for the Compound method when generating 250 m DEMs from the source 10 m DEM).

Fig. 5 shows the 3D surfaces for the different resolution DEMs (90, 150, and 250 m) generalized from the 30 m DEM using the three methods. These images show how the DEM surface generalized with ANUDEM looks much smoother (Fig. 5b) and that the Compound method (Fig. 5c) was able to retain more terrain

Table 2
RMSEs produced with different DEM generalization approaches.

Resolution (m)/Approach		10	30	50	90	125	150	250	500
3 m[a]	Stream Burning (m)	3.05	7.83	13.47	22.92	32.04	40.25	–	–
	ANUDEM (m)	4.86	11.42	16.33	25.66	33.90	42.42	–	–
	Compound (m)	**2.57**	**6.54**	**10.25**	**18.62**	**25.05**	**30.20**	–	–
10 m	Stream Burning (m)	–	**4.86**	**8.94**	15.71	24.48	34.58	51.85	–
	ANUDEM (m)	–	11.16	16.01	24.59	32.12	38.62	54.55	–
	Compound (m)	–	6.38	9.41	**15.61**	**22.79**	**30.04**	**45.82**	–
30 m	Stream Burning (m)	–	–	**9.11**	**15.50**	24.11	33.14	49.87	72.68
	ANUDEM (m)	–	–	15.66	23.96	31.82	38.12	54.44	78.31
	Compound (m)	–	–	9.76	15.65	**22.28**	**28.32**	**42.07**	**64.98**

[a] 3 m, 10 m and 30 m refer to the original DEMs. The lowest RMSEs are bold.

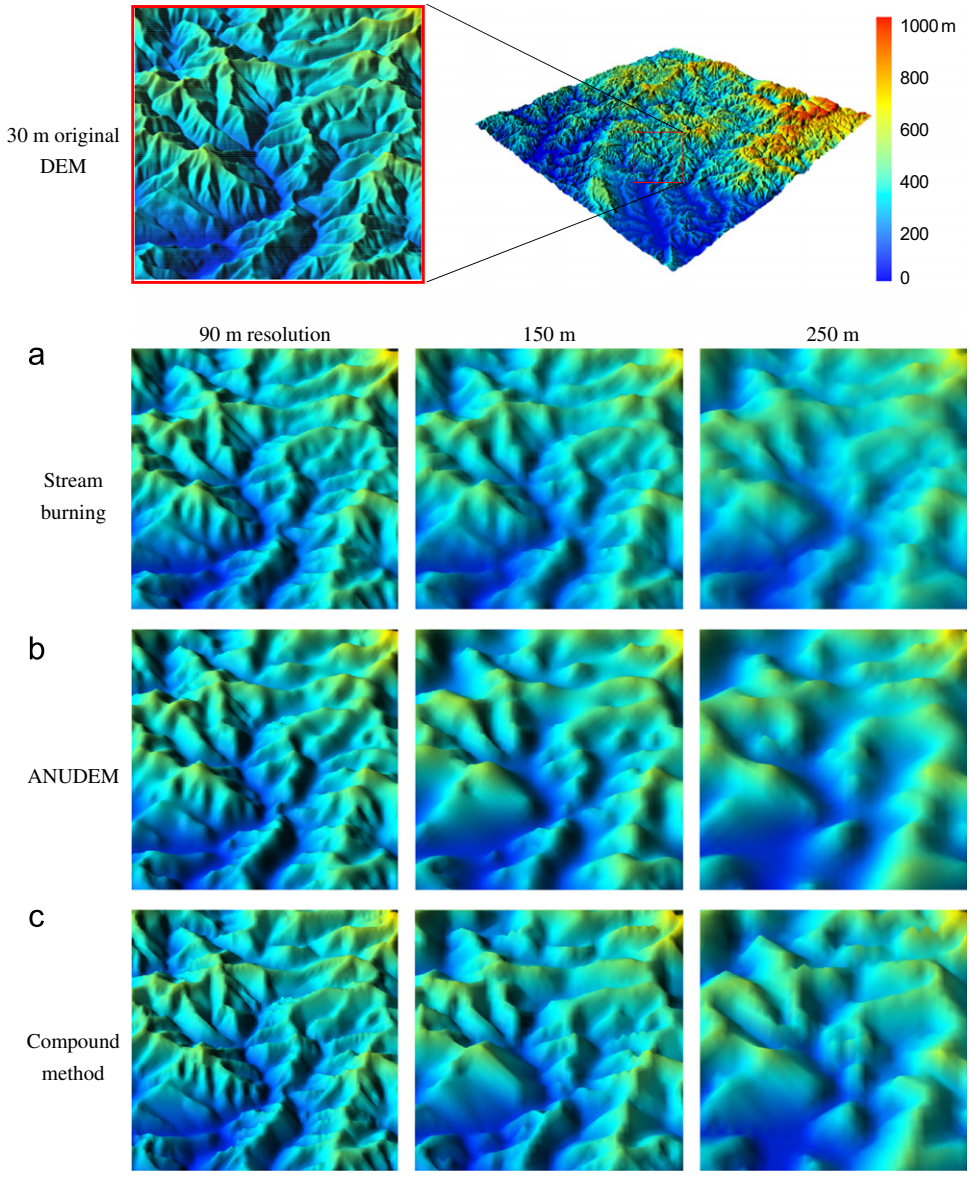

Fig. 5. 3D surfaces of DEMs generated from original 30 m DEM by three methods.

features at coarser resolutions than both ANUDEM and the Stream Burning algorithm (Fig. 5a).

3.2. Comparison of the mean slope and surface roughness values

Figs. 6 and 7 show the slopes for a sample of the different resolution DEMs generated with the three methods from the original 3 m and 30 m DEMs. The gradual changes in color show the gradual decline in slope and surface roughness as the DEM resolution was relaxed. In addition, a closer examination of the Stream Burning results reproduced in Figs. 6a and 7a shows the tendency for this method to increase slopes along the drainage lines (no doubt due to the 10 m descending depth used to 'retain' the drainage network). The slope maps generated with ANUDEM and reproduced in Figs. 6b–7b and the surface roughness results confirmed the previously noted tendency for this method to eliminate many significant slopes and much of the surface roughness (such that many terrain features were lost). The results for the Compound method reproduced in Figs. 6c–7c show this method performed well in preserving the slopes at low to moderate levels of generalization but that much of the detail was lost with this method (and the two previous methods) at high levels of generalization (as illustrated by the slope maps for the 250 m DEMs reproduced in Fig. 7 for example).

The superior performance of the Compound method is confirmed by the results shown in Tables 3 and 4. The results summarized in Table 3 show how the different methods produced slightly different mean slope values at relatively fine resolutions and that these discrepancies increased in magnitude at coarser resolutions because the mean slope values decreased half as much for the Compound method compared to the other two methods. The surface roughness results summarized in Table 4 show a similar pattern. Finally, the first entries in both Tables 3 and 4 show how the Stream Burning method generated larger mean slope and surface roughness values when the 10 m DEM was generated from the source 3 m DEM (due to the 10 m descending depth used to 'retain' the original drainage network).

3.3. Comparison of the SMR and SME values

Tables 5 and 6 show the streamline matching rate (SMR) and streamline matching error (SME) values produced with different

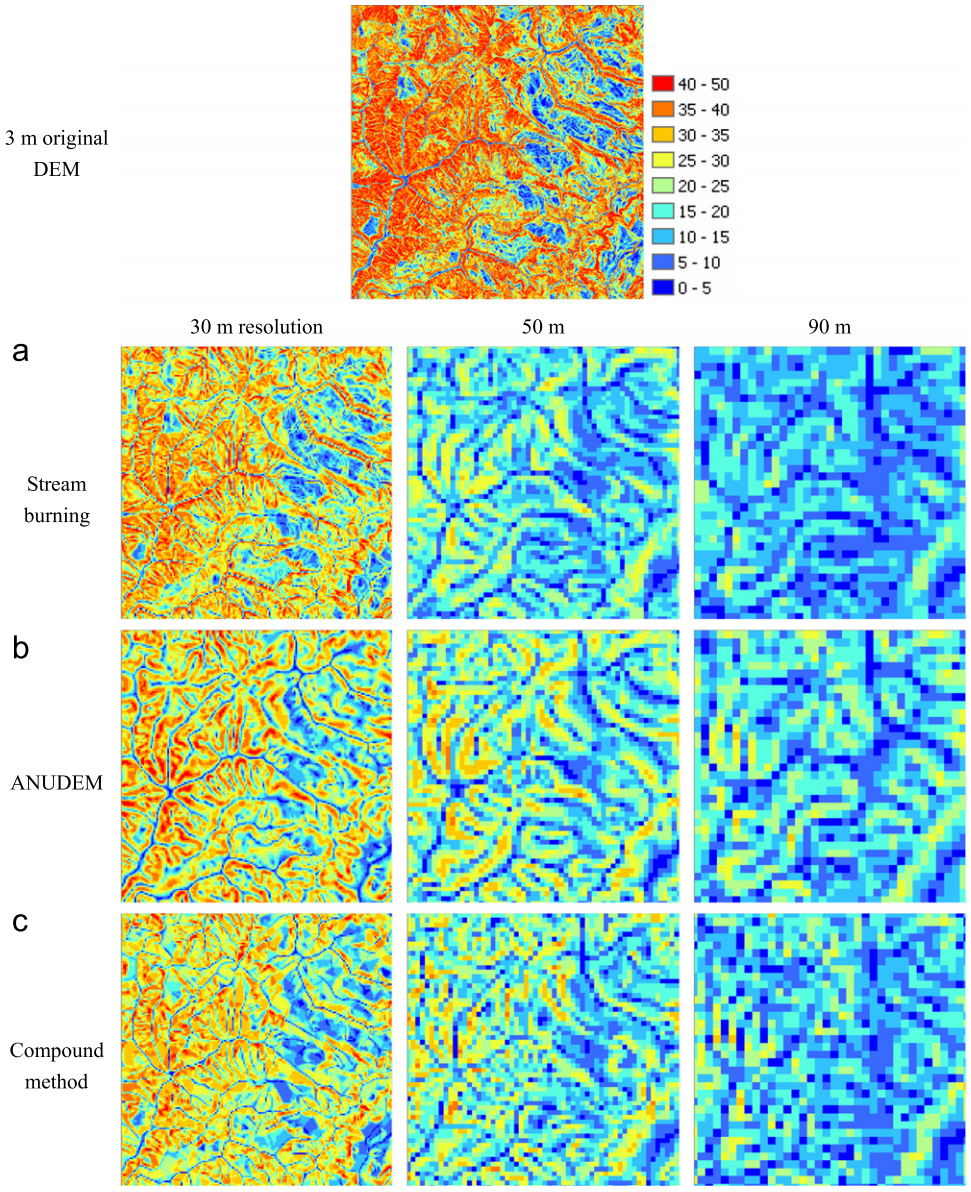

Fig. 6. The slope of DEMs generated from original 3 m DEM by three methods.

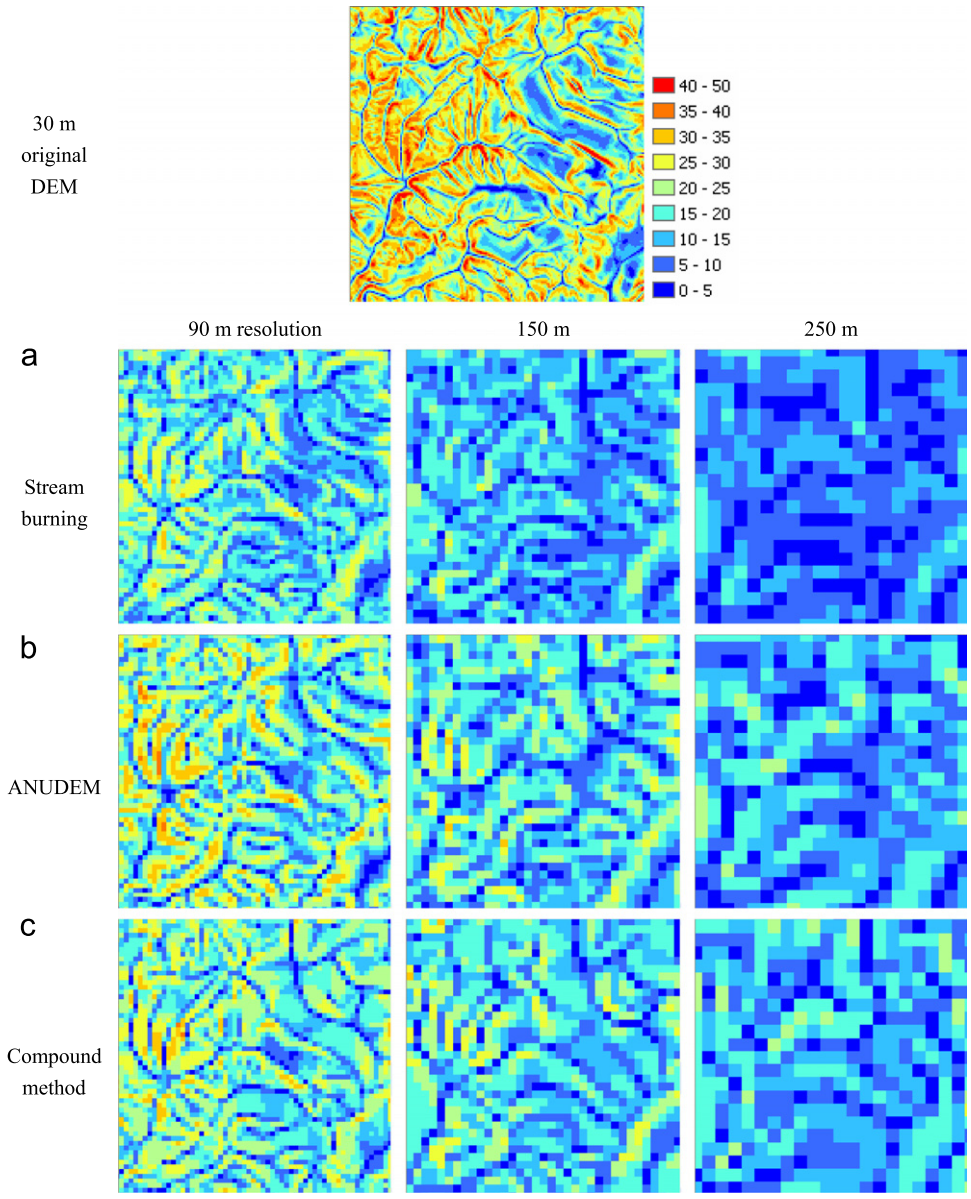

Fig. 7. The slope of DEMs generated from original 30 m DEM by three methods.

Table 3
The mean slope values produced with different DEM generalization approaches.

Resolution (m)/Approach		10	30	50	90	125	150	250	500
3 m[a](28.72°)	Stream Burning (°)	29.62	26.32	23.62	19.56	16.87	15.33	–	–
	ANUDEM (°)	27.34	24.59	22.32	18.81	16.48	14.99	–	–
	Compound (°)	**28.52**	**27.80**	**27.00**	**25.08**	**22.90**	**21.02**	–	–
10 m (22.86°)	Stream Burning (°)	–	22.35	20.81	18.00	15.97	14.77	11.29	–
	ANUDEM (°)	–	21.05	19.64	17.26	15.54	14.39	11.45	–
	Compound (°)	–	**22.92**	**22.64**	**21.83**	**20.69**	**19.53**	**16.69**	–
30 m (21.23°)	Stream Burning (°)	–	–	20.08	17.46	15.50	14.33	11.02	7.15
	ANUDEM (°)	–	–	18.74	16.58	15.00	14.01	11.44	8.05
	Compound (°)	–	–	**21.72**	**20.97**	**19.98**	**18.91**	**16.67**	**13.71**

[a] The mean slopes of the original 3 m, 10 m and 30 m DEMs were 28.72°, 22.86° and 21.23°, respectively.

DEM generalization approaches. Two general trends are evident: the SMR values gradually decrease and SME values increase with each method and source DEM with successively higher levels of generalization.

These trends were most pronounced for the Stream Burning algorithm for which the results started off reasonably well at high spatial resolutions but deteriorated quickly beyond the initial generalization step. The streamline matching rate fell below 50%

Table 4
The surface roughness values produced with different DEM generalization approaches.

Resolution (m)/Approach		10	30	50	90	125	150	250	500
3 m[a] (1.182)	Stream Burning	**1.189**	1.142	1.113	1.075	1.056	1.046	–	–
	ANUDEM	1.160	1.126	1.102	1.071	1.054	1.044	–	–
	Compound	1.173	**1.161**	**1.151**	**1.132**	**1.114**	**1.098**	–	–
10 m (1.118)	Stream Burning	–	1.107	1.091	1.067	1.052	1.044	1.026	–
	ANUDEM	–	1.096	1.079	1.060	1.047	1.041	1.022	–
	Compound	–	**1.113**	**1.109**	**1.101**	**1.091**	**1.083**	**1.065**	–
30 m (1.097)	Stream Burning	–	–	1.085	1.063	1.049	1.042	1.025	1.010
	ANUDEM	–	–	1.074	1.057	1.047	1.041	1.027	1.013
	Compound	–	–	**1.098**	**1.092**	**1.084**	**1.076**	**1.062**	**1.045**

[a] The surface roughness of the original 3 m, 10 m and 30 m DEMs were 1.182, 1.118 and 1.097, respectively.

Table 5
The SMR values produced with different DEM generalization approaches.

Resolution (m)/Approach		10	30	50	90	125	150	250	500
3 m	Stream Burning (%)	88.3	54.5	36.6	23.5	15.2	9.6	–	–
	ANUDEM (%)	81.4	65.9	58.3	51.6	48.0	45.2	–	–
	Compound (%)	**91.6**	**78.3**	**67.3**	**58.1**	**51.5**	**47.5**	–	–
10 m	Stream Burning (%)	–	87.5	56.6	37.9	25.3	19.5	10.7	–
	ANUDEM (%)	–	80.6	68.8	61.3	57.7	54.8	50.9	–
	Compound (%)	–	**90.1**	**82.5**	**73.2**	**67.1**	**62.9**	**53.4**	–
30 m	Stream Burning (%)	–	–	88.0	65.8	46.1	37.5	22.3	11.6
	ANUDEM (%)	–	–	78.5	71.2	66.3	63.5	60.2	57.7
	Compound (%)	–	–	**89.8**	**82.8**	**76.6**	**72.1**	**67.5**	**60.3**

Table 6
The SME values produced with different DEM generalization approaches.

Resolution (m)/Approach		10	30	50	90	125	150	250	500
3 m	Stream Burning (m)	3.1	8.0	15.5	24.1	33.4	40.7	–	–
	ANUDEM (m)	4.3	6.5	8.1	9.6	10.7	11.8	–	–
	Compound (m)	**2.8**	**4.7**	**6.2**	**8.1**	**9.7**	**11.0**	–	–
10 m	Stream Burning (m)	–	11.5	26.0	38.2	47.9	55.1	66.5	–
	ANUDEM (m)	–	14.4	18.7	21.9	25.5	23.7	29.6	–
	Compound (m)	–	**10.2**	**13.5**	**17.2**	**19.5**	**21.3**	**26.6**	–
30 m	Stream Burning (m)	–	–	16.9	38.9	55.3	61.8	85.8	120.2
	ANUDEM (m)	–	–	25.7	32.1	37.0	40.2	44.5	50.5
	Compound (m)	–	–	**15.3**	**21.1**	**26.4**	**29.0**	**35.5**	**45.2**

after just two generalization steps for all three source DEMs (Table 5) and the streamline matching errors grew five-fold or more across the six generalization levels (Table 6). The results for the ANUDEM method show how this method performed the worst at the first generalization level for each of the source DEMs but that its performance recovered thereafter and closely tracked that of the Compound method, such that this method performed well in preserving drainage features in the coarser DEMs. However, the results reproduced in Tables 5 and 6 show how the Compound method produced the best matching and smallest error rates for the drainage features for all 18 combinations of generalization levels and source DEMs. This result can be explained by the additional drainage-constrained edges that were incorporated in the TIN generation process in this instance (see Zhou and Chen (2011) for additional details).

4. Conclusions

In this study, we compared the capabilities of three drainage-constrained methods—the Stream Burning algorithm of Saunders (2000), ANUDEM (Hutchinson, 1989) and the Compound Constrained-TIN approach of Zhou and Chen (2011)– in retaining inherent morphological and drainage features. Five characteristics of the morphological and drainage features of fluvial terrain surfaces–the elevation, slope, surface roughness, streamline matching rate (SMR) and streamline matching error (SME) were used for the comparisons.

The results show that the stream burning method changed the terrain surface significantly and produced unacceptable errors for most of the terrain derivatives. This method performed poorly in retaining drainage features for coarser resolution generalized DEMs. Compared with the stream burning method, ANUDEM performed much better in preserving the key morphological and hydrological features. However, ANUDEM relies on a surface fitting approach to generate the terrain surface, and this caused substantial smoothing and the loss of detail in most of the experiments. The Compound method consistently delivered the best results among the three algorithms. This method supplemented the maximum z-tolerance algorithm with drainage feature lines, to construct a drainage-constrained TIN. The results show that the Compound method was able to retain the terrain surface and accompanying drainage features better than the aforementioned approaches across a variety of generalization

levels. However, all three methods did relatively poorly at high levels of generalization such as when a 500 m DEM was generated from a 30 m source DEM.

Future work will focus on two kinds of improvements. The first is the consideration of other flow routing algorithms given the numerous studies that have documented that the simple D8 algorithm (used for the work at hand) may not be the best method to retrieve drainage networks in some fluvial kinds of landscapes. The second extension will be to explore the effects of drainage-constrained generalization methods on other morphological and drainage parameters, such as slope length, curvatures, stream length and catchment area, which are important for a variety of practical applications.

Acknowledgments

The research is supported by grants from the National Key Basic Research and Development Program (no: 2012CB719906), the National Nature Science Foundation of China (no: 41171347), and the Hong Kong Baptist University Faculty Research Grant (no: FRG/11-12/030).

References

Ai, T., Li, J., 2010. A DEM generalization by minor valley branch detection and grid filling. ISPRS Journal of Photogrammetry and Remote Sensing 65 (2), 198–207.

Belhadj, F., Audibert, P., 2005. Modeling landscapes with ridges and rivers: bottom up approach. In: GRAPHITE '05: Proceedings of the 3rd International Conference on Computer Graphics and Interactive Techniques in Australasia and South East Asia, pp. 447–450.

Callow, J.N., van Niel, K.P., Boggs, G.S., 2007. How does modifying a DEM to reflect known hydrology affect subsequent terrain analysis? Journal of Hydrology 332 (1–2), 30–39.

Chang, K., 2007. Introduction to Geographic Information Systems, 4th edition McGraw-Hill, New York 450pp.

Danovaro, E., De Floriani, L., Papaleo, L., Vitali, M., 2006. A multi-resolution representation for terrain morphology. In: Raubal, M., Miller, H., Goodchild, M.F. (Eds.), GIScience 2006, Lecture Notes in Computer Science 4197. Münster, Germany, pp. 33–46.

Douglas, D.H., Peucker, T.K., 1973. Algorithms for the reduction of the number of points required to represent a digitized line or its caricature. Canadian Cartographer 10 (2), 112–122.

Douglas, D.H, 1986. Experiments to locate ridges and channels to create a new type of digital elevation model. Cartographica 23 (4), 29–61.

Fowler, R.J., Little, J.J., 1979. Automatic extraction of irregular network digital terrain models. ACM SIGGRAPH Computer Graphics 13 (2), 199–207.

Gesch, D.B., 1999. The effects of DEM generalization methods on derived hydrologic features. In: Lowell, K., Jaton, A. (Eds.), Spatial Accuracy Assessment: Land Information Uncertainty in Natural Resources. Ann Arbor Press, Chelsea, Michigan, pp. 255–262.

Heller, M., 1990. Triangulation algorithms for adaptive terrain modelling. In: Proceedings of the 4th International Symposium on Spatial Data Handling, Zürich, vol. 1, pp. 163–174.

Hutchinson, M.F., 1989. A new procedure for gridding elevation and streamline data with automatic removal of spurious pits. Journal of Hydrology 106, 211–232.

Jenson, S.K., Domingue, J.O., 1988. Extracting topographic structure from digital elevation data for geographic information system analysis. Photogrammetric Engineering and Remote Sensing 54 (11), 1593–1600.

Kidner, D.B., Ware, J.M., Sparkes, A.J., Jones, C.B., 2000. Multiscale terrain and topographic modelling with the implicit TIN. Transactions in GIS 4 (4), 379–408.

Kienzle, S., 2004. The Effect of DEM Raster Resolution on First Order, Second Order and Compound Terrain Derivatives. Transactions in GIS 8 (1), 83–111.

Lee, J., 1991. Comparison of existing methods for building triangular irregular network models of terrain from grid digital elevation models. International Journal of Geographical Information Systems 5 (3), 267–285.

Li, Z., 2008. Multi-scale digital terrain modelling and analysis. In: Zhou, Q., Lees, B., Tang, G. (Eds.), Advances in Digital Terrain Analysis. Springer, Berlin, pp. 59–83.

Mark, D.M., 1984. Automatic detection of drainage networks from digital elevation models. Cartographica 21 (2–3), 168–178.

Nelson, E.J., Jones, N.L., Berrett, R.J., 1999. Adaptive tessellation method for creating TINs from GIS data. Journal of Hydrologic Engineering 4 (1), 2–9.

Peucker, T.K., Douglas, D.H., 1975. Detection of surface-specific points by local parallel processing of discrete terrain elevation data. Computer Graphics and Image Processing 4, 375–387.

Saunders, W., 2000. Preparation of DEMs for use in environmental modelling analysis. In: Maidment, D., Djokic, D. (Eds.), Hydrologic and hydraulic modelling support with geographic information systems. Redlands, Environmental Systems Research Institute Inc, pp. 29–51.

Soille, P., Vogt, J.V., Colombo, R., 2003. Carving and adaptive drainage enforcement of grid digital elevation models. Water Resources Research 39 (12), 1366–1379.

Southard, D.A., 1991. Piecewise planar surface models from sampled data. In: Patrikalakis, N.M. (Ed.), Scientific visualization of physical phenomena. Springer-Verlag, Tokyo, pp. 667–680.

Tay, L.T., Sagar, B.S.D., Chuah, H.T., 2005. Analysis of geophysical networks derived from multiscale digital elevation models: a morphological approach. IEEE Geoscience and Remote Sensing Letters 2 (4), 399–403.

Vázquez, J.P., Pascual, J.P., 2008. Automated spot heights generalization in trail maps. International Journal of Geographical Information Science 22 (1), 91–110.

Weibel, R., 1992. Models and experiments for adaptive computer-assisted terrain generalization. Cartography and Geographic Information Systems 19 (3), 133–153.

Wilson, J.P., Gallant, J.C., 2000. Terrain Analysis: Principles and Applications. John Wiley & Sons, New York 479pp.

Wise, S.M., 2000. Assessing the quality of hydrological applications of digital elevation models derived from contours. Hydrological Processes 14, 1909–1929.

Wolock, D.M., Price, C.V., 1994. Effects of digital elevation model and map scale and data resolution on a topography-based watershed model. Water Resources Research 30 (11), 3041–3052.

Wu, J., Amaratunga, K., 2003. Wavelet triangulated irregular networks. International Journal of Geographical Information Science 17 (3), 273–289.

Wu, S., Li, J., Huang, G.H., 2008. Characterization and evaluation of elevation data uncertainty in water resource modeling with GIS. Water Resources Management 22 (8), 959–972.

Zakšek, K., Podobnikar, T., 2005. An effective DEM generalization with basic GIS operations. In: Proceedings of the 8th I.C.A. Workshop on Generalization and Multiple Representation, A Coruña, Spain, 10 pp. (on CD-ROM).

Zhang, X., Drake, N.A., Wainwright, J., Mulligan, M., 1999. Comparison of slope estimates from low resolution DEMs: scaling issues and a fractal method for their solution. Earth Surface Processes and Landforms 24 (9), 763–779.

Zhou, Q., Chen, Y., 2011. Generalization of DEM for terrain analysis using a compound method. ISPRS Journal of Photogrammetry and Remote Sensing 66 (1), 38–45.

Zhou, Q., Liu, X., 2004. Analysis of errors of derived slope and aspect related to DEM data properties. Computers and Geosciences 30 (4), 369–378.